Bull. Inst. Chem. Res., Kyoto Univ., Vol. 73, No. 1, 1995

System of the 100 MeV Electron Injector for the KSR

Toshiyuki SHIRAI*, Hideki DEWA*, Hirokazu FUJITA*, Masaki KANDO*, Masanori IKEGAMI*, Yoshihisa IWASHITA*, Shigeru KAKIGI*, Akira NODA*, Katsuo MASHIKO** and Makoto INOUE*

Received February 7, 1995

A 100 MeV electron linear accelerator has been constructed at the Institute for Chemical Research, Kyoto University. It is an electron injector for the 300 MeV electron storage ring (KSR). The electron injector consists of the electron gun, buncher and three disc-loaded accelerating waveguides. The accelerating waveguide is operated at 2857 MHz and 3 m long in length. The output beam energy from the injector is 100 MeV and the designed beam current is 100 mA.

KEY WORDS: Linear accelerator/ Electron injector/ Storage ring/ Synchrotron radiation

1. INTRODUCTION

A compact electron storage ring (Kaken Storage Ring, KSR) is now under construction at the Institute for Chemical Research, Kyoto University[1]. It will be used for the synchrotron radiation source. The ring accelerates the electron beam up to 300 MeV. The critical wave length of the synchrotron radiation from the dipole magnet is 17 nm. An electron linear accelerator is used as the injector for the KSR. The layout of the electron linac and the KSR is shown in Fig. 1. The electron linac was originally installed at the Japan Atomic Energy Research Institute (JAERI) and had been used for the neutron physics[2,3]. It was shut down at

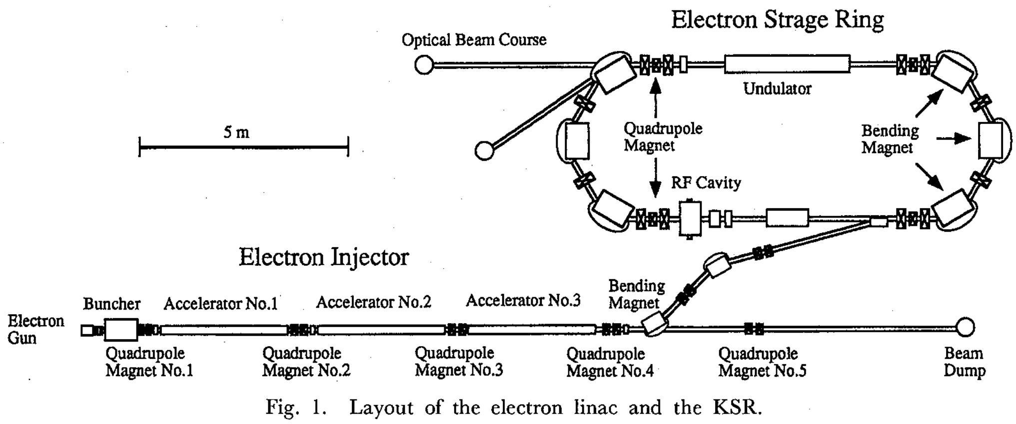

Fig. 1. Layout of the electron linac and the KSR.

* 白井敏之, 出羽秀紀, 冨士田浩一, 神門正城, 池上雅紀, 岩下芳久, 柿木　茂, 野田　章, 井上　信 : Nuclear Science Research Facility, Institute for Chemical Research, Kyoto University
** 益子勝夫 : Nihon Kensetsu Kogyo Co Ltd.

1993. Main components of the JAERI linac were transported from JAERI to the Kyoto University for the KSR project.

The main parameters of the injector are listed in Table 1. The higher injection energy is desirable to obtain the good accumulation condition because the damping time becomes shorter and the beam life becomes longer into the KSR. But the size of the injector becomes larger. The injection energy of 100 MeV is decided from the above reasons. The beam pulse width of 1 μsec is 3 times longer than the revolution time of the KSR. It enables the multi turn injection into the KSR. The high beam current is desirable but the heavy beam loading leads to the large energy spread. Our aim is to get the beam current of 100 mA within the energy spread of $\pm 0.5\%$. The repetition of 20 Hz is limited by the capability of the power supply and the radiation shield. It is enough high for the KSR injection because the repetition of the beam injection should be less than 1 Hz.

Table 1. Main parameters of the injector.

Output Beam Energy	100 MeV
Energy Spread	$\pm 0.5\%$
Beam Current	100 mA
Beam Pulse Width	1 μsec
Max. Repetition	20 Hz

2. LOW ENERGY SECTION

The electron linac is divided into two sections. One is a low energy section, the other is a high energy section. The former generates the electron beam and bunches it. The latter accelerates the electron beam up to 100 MeV and transports it to the KSR or to the beam dump. The low energy section consists of an electron gun, a pre-buncher, a buncher and focusing coils. The layout of the low energy section is shown in Fig. 2.

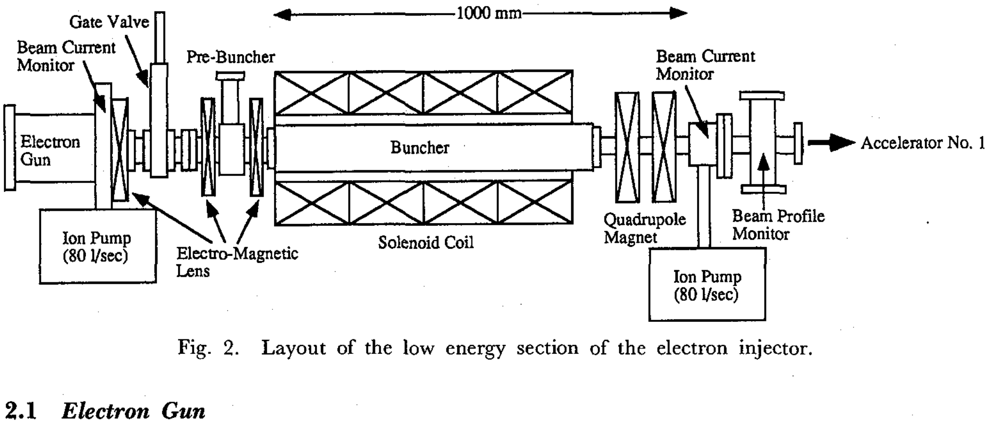

Fig. 2. Layout of the low energy section of the electron injector.

2.1 *Electron Gun*

The electron gun is a Pierce type gridded gun. The electron beam from the cathode is focused by the electric field between the cathode and anode. The cathode assembly is a Y-796 (Eimac). The block diagram of the power supply system for the electron gun is shown in Fig. 3. The maximum extraction voltage is -100 kV DC. The filament voltage is 6 V. The grid bias voltage is 50 V and the pulsed grid voltage is -100 V in the usual operation. The pulse width of the grid voltage is variable from 10 nsec to 1 μsec.

2.2 *Pre-buncher*

The pre-buncher is a single re-entrant cavity. The maximum input power is 120 kW and the resonant frequency is 2857 MHz at 35°C. It is designed to compress the phase spread within 60 degree. The buncher is a disc-loaded and 3 step constant gradient type. It has 21 cells and the total length is 777 mm. The maximum input power is 12 MW. The designed phase spread is within 3 degree at the beam current of 100 mA.

2.3 *Focusing Coil*

The strong and continuous focusing force is needed to transport the low energy electron beam because the space charge repulsion is very strong. Three electro-magnetic lenses are installed in the low energy section. They focus the beam and reduce the beam loss. The buncher is surrounded by the four solenoid coils. They produce the axial magnetic field of 1.5 kGauss along the beam axis and keep the beam size constant in the buncher.

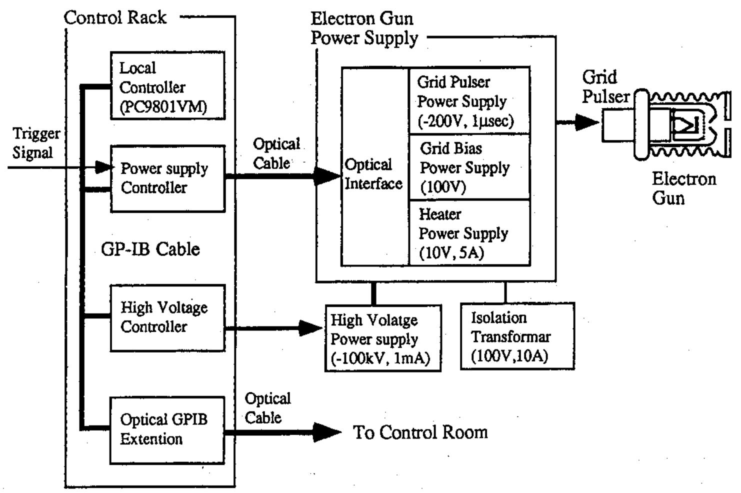

Fig. 3. Schematic block diagram of the power supply system for the electron gun.

3. HIGH ENERGY SECTION

3.1 *Accelerating Waveguide*

The high energy section consists of the three accelerating waveguides and the quadrupole magnets between them. The view of the accelerating waveguide and the klystron are shown in photo 1. The main characteristics of the accelerating waveguides are listed in Table 2. The accelerating waveguide is a constant gradient type. The relation between the energy gain of the electron (E) and the beam current (I) is

$$E=\sqrt{PLr}(1-e^{-2\tau})-\frac{Lr}{2}I\left(1-\frac{2\tau e^{-2\tau}}{1-e^{-2\tau}}\right), \tag{1}$$

where P is a input RF power, L is a length of the accelerating waveguide, r is a shunt impedance

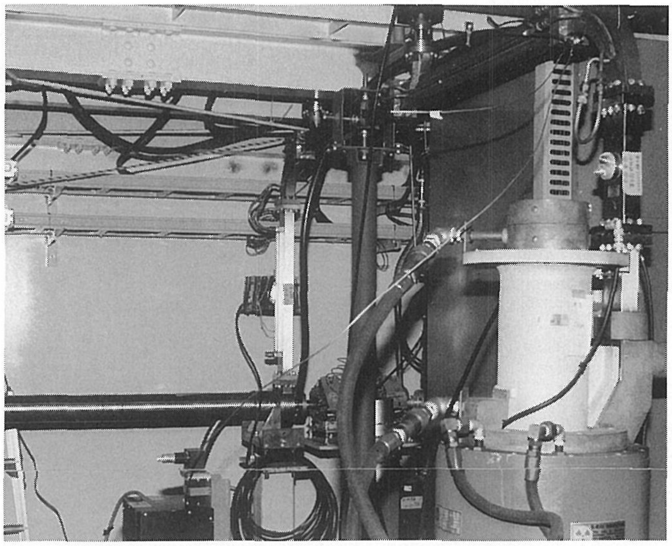

Photo 1. View of the accelerating waveguide and the klystron.

and τ is an attenuation factor. Figure 4 shows the relation at the various input power. The beam loading is 3.6 MeV at the beam current of 100 mA. It means that the energy spread of $\pm 4\%$ occurred within 1 pulse. The transient mode acceleration is considered to obtain the smaller energy spread.

3.2 *Quadrupole Magnet*

The space charge repulsion is negligible in the high energy section because the electron energy is over 3 MeV after the buncher. The doublet of the quadrupole magnets is used

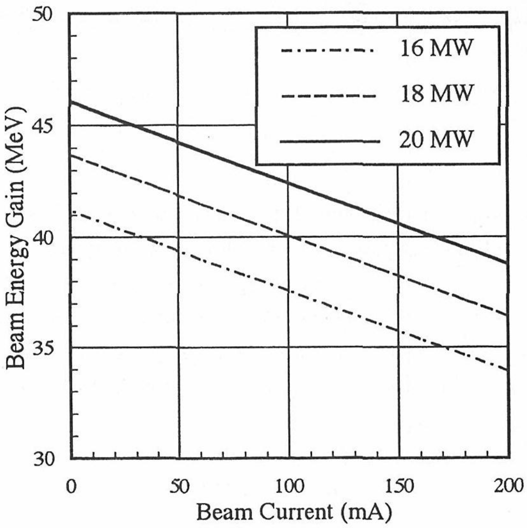

Fig. 4. Relation between the beam energy gain (E) and the beam current (I) in the accelerating waveguide.

Table 2. Main characteristics of the accelerating waveguide.

Mode	2/3 π, Constant Gradient
Number of Cell	85
Bore Radius	11.74–13.4 mm
Length	3 m
Operating Frequency	2857 MHz at 35°C
Input power	20 MW (pack)
VSWR	<1.05
Shunt Impedance	53 MΩ/m
Maximum Electric Field	15 MV/m
Attenuation Factor	0.56

between the accelerating waveguides as a focusing element. The magnetic field gradient of the quadrupole magnet is 300 Gauss/cm. The pole length is 40 cm (Q-mag. No.1) or 80 cm and the bore radius is 21 mm. The calculated beam radius along the beam axis is shown in Fig. 5. It is assumed that the normalized emittance is 100 π·mm·mrad. The focusing strength of the quadrupole magnets is enough high to avoid the beam loss.

The steering coils are placed at the entrance of the first and the third accelerating waveguides to correct the beam direction.

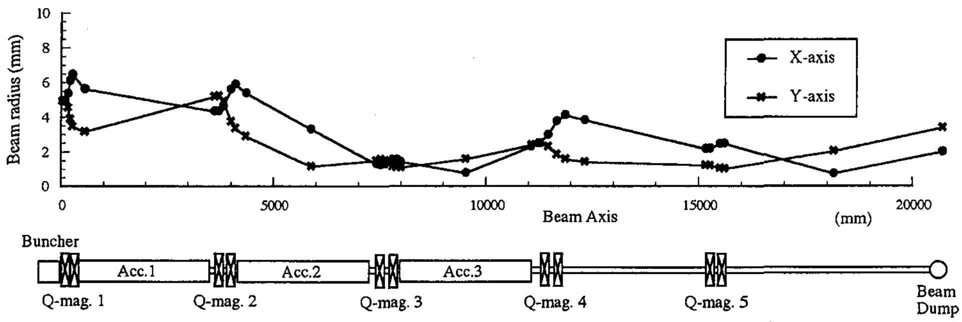

Fig. 5. Calculated beam radius along the beam axis. The normalized emittance is assumed to be 100 π·mm·mrad.

3.3 *Beam Dump*

A beam window is attached at the end of the beam transport. The electron beam is injected to the beam dump through the window. The window is made of the Ti foil with the thickness of 0.05 mm. The schematic view of the beam dump is shown in Fig. 6. The beam is stopped by the Fe target. The thickness of the Fe target is 15 cm and it can stop the electro-magnetic cascade shower induced by the electron beam. The target is surrounded by the Pb block with the thickness of 20 cm to reduce the X-ray. The concrete shield blocks are placed around the beam dump to absorb the neutron.

4. RF SYSTEM

4.1 *RF Low Power System*

The block diagram of the RF system is shown in Fig. 7. The master RF oscillator is a

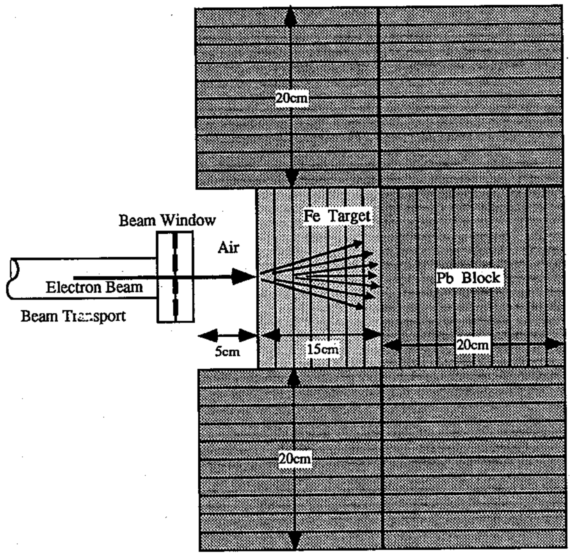

Fig. 6. Schematic view of the beam dump.

synthesized signal generator (HP-8664A). It has a good frequency stability of 1.5×10^{-8} per a day. The output power of 2 W from the solid state amplifier is supplied into the booster klystron in the accelerator room through a coaxial cable (8D-SFA, Fujikura). The length of the cable is about 40 m and the cable loss is about −10 dB.

The booster klystron (TH-2436, Thomson) has a gain of 40 dB and the output power is 10 kW. The pulse width is 3.5 μsec. The output power is divided by the 4-way RF divider and supplied to the four main klystrons. There are RF attenuators and phase shifters before the main klystrons. They control the RF amplitude and phase to achieve the optimum beam acceleration.

4.2 *Klystron and Waveguide*

The main klystron is ITT-8568. The main characteristics of the klystron are shown in Table 3. The maximum output power is 21 MW and the minimum input power is 105 W. The optimum frequency is tuned at 2856 MHz.

The RF power is supplied from the klystron into the accelerating waveguide through the waveguide. The inside of the waveguide is evacuated to avoid the discharge. The output RF power from the accelerating waveguide is absorbed by a water loaded dummy load. The waveguide between the accelerating waveguide and the dummy load is pressurized with the N_2

Table 3. Main characteristics of the main klystron (ITT-8568).

Heater	15 V, 14 A
Operating Frequency	2856 MHz
Cathode Voltage	250 kV
Beam Current	250 A
Input RF Power	105 W
Output RF Power	21 MW
Power Gain	53 dB

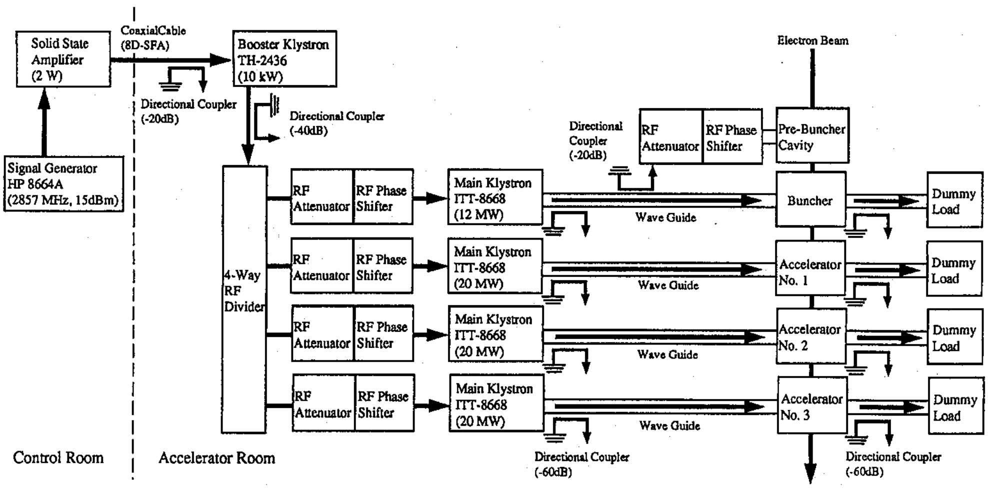

Fig. 7. Schematic block diagram of the RF system.

gas because of the discharge consideration.

Some directional couplers are installed in the RF system. The RF signal is detected by a RF diode at the monitor rack and it is observed in the control room.

4.3 *Modulator*

The modulator supplies the high voltage pulse to the klystron. The main circuit of the klystron power supply is shown in Fig. 8. It is composed of the high voltage power supply, the pulse forming network (PFN) and the pulse transformer. The generated pulse voltage of the PFN is up to 22.5 kV and the peak current is 3,000 A. The pulse width is 2 μsec. The output voltage is stepped up 12 times higher by the pulse transformer and supplied to the klystron.

There are two high voltage power supplies and the four PFNs and four pulse transformers.

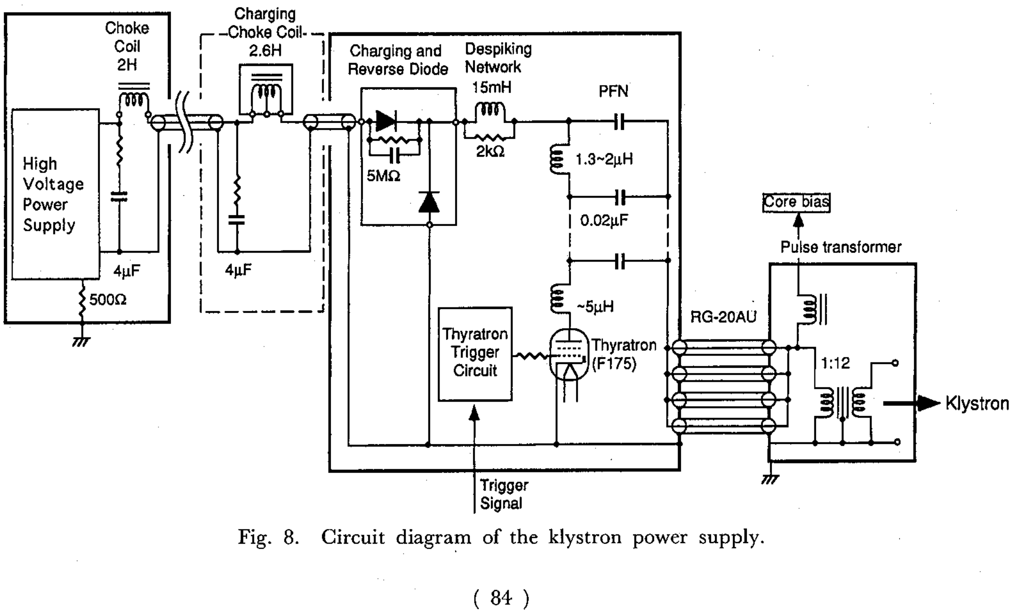

Fig. 8. Circuit diagram of the klystron power supply.

The maximum output voltage of the high voltage power supply is 25 kV DC. One high voltage power supply of which the maximum output current 250 mA DC, is connected to the PFN and the pulse transformer for the buncher. The other of which the maximum output current 500 mA DC, is connected to the three PFNs and the pulse transformers for the three accelerating waveguides.

5. BEAM MONITOR

5.1 *Beam Current Monitor*

Figure 9 shows the position of the beam monitors. The current monitor is a core monitor. The core is made of a ferrite (2000L, Tohoku Metal Industries). The number of coil turns is 30. The current sensitivity is 1 mV/mA.

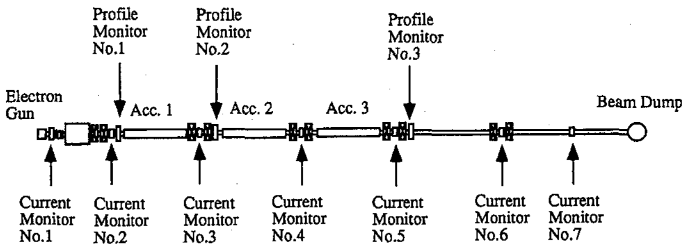

Fig. 9. Position of the beam current monitors and the profile monitors.

5.2 *Beam Profile Monitor*

The beam profile monitors will be installed in the beam line. The position of the beam profile monitors is also shown in Fig. 9. The material of the beam screen is an alumina ceramic in which a little chromium oxide is homogeneously doped (Desmarquest, AF995R)[4]. The fluorescence is observed by a CCD camera. The beam profile monitor is used for the emittance measurements with a slit or a pepper pot plate.

6. VACUUM SYSTEM

The schematic block diagram of the vacuum system is shown in Fig. 10. All of the vacuum pumps of the injector are sputter ion pumps. A turbo molecular pump is used only for the rough pumping. One or two sputter ion pumps (10 *l*/sec) are attached on each waveguide. Main sputter ion pumps (80 *l*/sec) are attached on the beam chamber about every 4 m. The vacuum pressure is observed by the ion current of the sputter ion pump and it is less than 1×10^{-8} Torr.

The klystron has a embedded sputterion pump (RCA-VC2119V8). The pumping speed is 10 *l*/sec and the usual vacuum pressure is less than 1×10^{-8} Torr.

7. CONTROL SYSTEM

7.1 *Trigger System*

The trigger system is necessary because each element in the injector has to work synchronously. Figure 11 shows the block diagram of the trigger system. The trigger pulses are supplied to the grid pulser of the electron gun and the trigger circuit of the monitor units. In

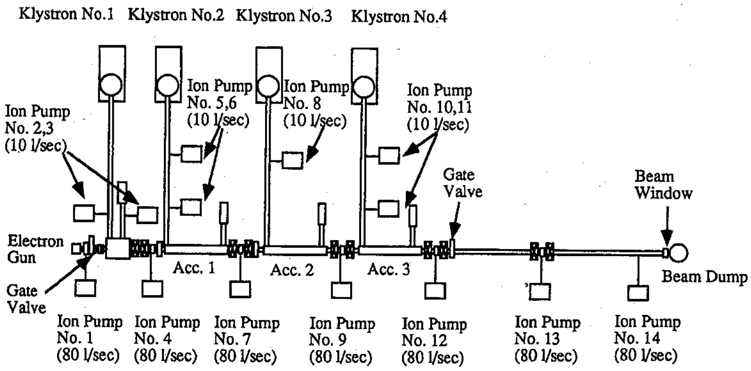

Fig. 10. Layout of the vacuum system.

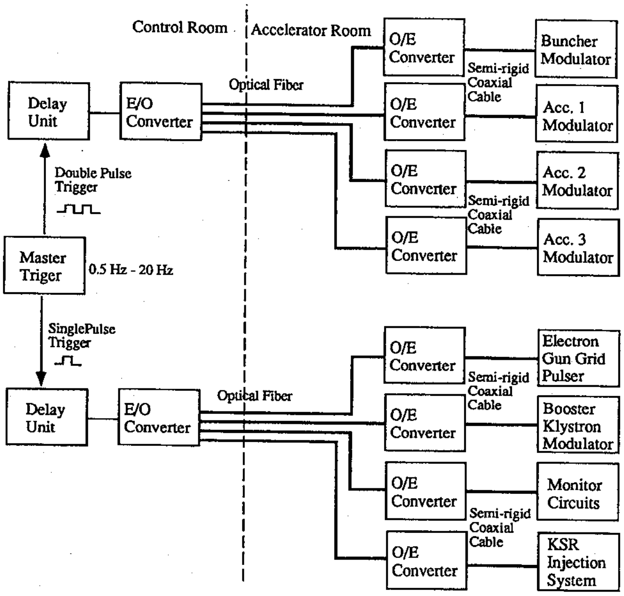

Fig. 11. Schematic block diagram of the trigger system.

the modulator, the thyratron SCR pulser accepts the trigger pulse and ignites the thyratron.

The master trigger generates two kinds of pulses with the variable repetition from 0.5 Hz to 20 Hz. One is a single mode pulse and the other is a double mode pulse with the pulse separation of 1 msec. The latter is needed for the modulator at the low repetition rate because the voltage at the PFN capacitors decreases after resonant charging.

The trigger pulses are transmitted through the optical fiber. It isolates the each section and reduces the noise.

7.2 *Device Control System*

The block diagram of the device control system is shown in Fig. 12. Each device is controlled by the GP-IB system. Some optical GP-IB extensions are used for the isolation of each device. The GP-IB controller is a personal computer IBM-PC/AT with ISA GP-IB card (AT-GPIB, National Instrument). The control software is worked on the Microsoft Windows

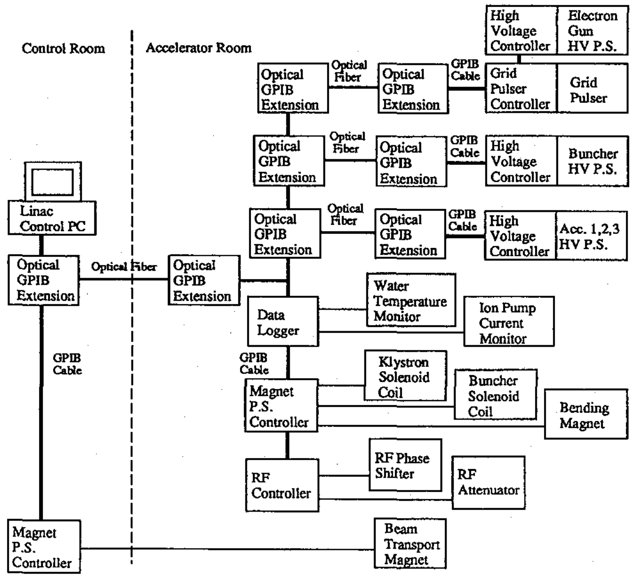

Fig. 12. Schematic block diagram of the control system.

system. The user can operate by the mouse or a touch panel.

7.3 *Interlock System*

The block diagram of the interlock control is shown in Fig. 13. The external interlock includes the door status of the accelerator room, the operation status of the proton linac and the radiation level. The emergency interlock includes the emergency stop button.

The interlock information are collected by the interlock monitors. Some devices are connected to the interlock monitors through the optical fiber to reduce the noise. The interlock monitor sends the signal to the interlock output module when the interlock information enters. It keeps the status until the reset signal is supplies. The interlock output module generates the

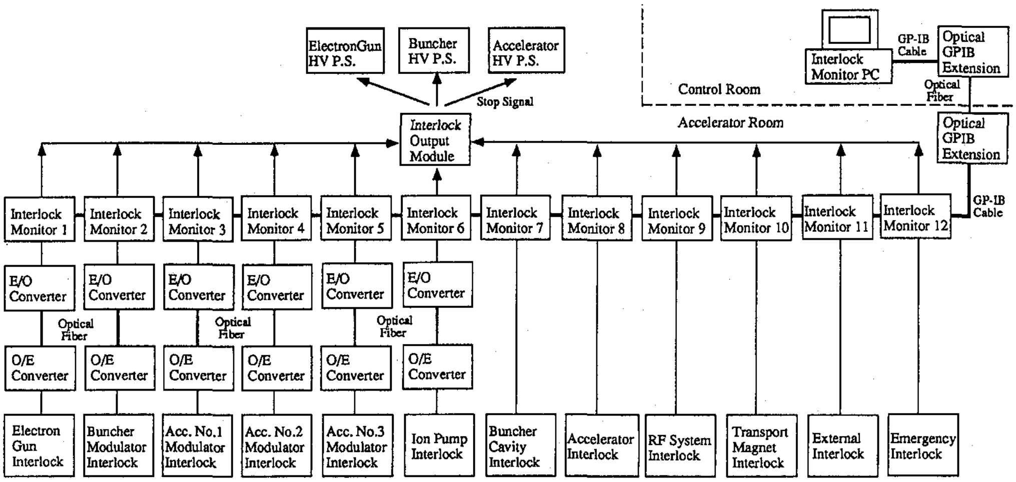

Fig. 13. Schematic block diagram of the interlock system.

stop signal to the high voltage power supply for the electron gun or the modulators. A personal computer reads interlock status from the interlock monitors via the GP-IB system. The operator can monitor the interlock status and reset by the computer.

8. UTILITIES

8.1 *Cooling Water*

There are two cooling water system (I, II). The water temperature of the cooling water system (I) is controlled and kept at 35.0°C. It is used to cool the accelerator cavity because the resonant frequency of the cavity is changed by 50 kHz per 1°C. The diameter of the main pipe is 50 mm and the diameter of the pipe to each accelerating waveguide is 25 mm. The water pressure is 5 kgf/cm^2 at the main valve.

The water temperature of the cooling water system (II) is not controlled. It cools the klystron system and the focusing coils. The diameter of the main pipe is 80 mm and the diameter of the pipe to each klystron is 50 mm. The water pressure is 5 kgf/cm^2 at the main valve.

8.2 *N_2 Gas*

The waveguide between the accelerating waveguide and the dummy load is pressurized with the N_2 gas. The waveguide between the buncher and the klystron is also pressurized with the N_2 gas. The N_2 gas is provided from the 40 liter gas tank through the copper tube. The gas pressure is 3 kgf/cm^2.

8.3 *Electrical*

There are 100 V–5 kVA, 200 V–50 kVA and 200 V–30 kVA board supplies in the accelerator room. The 100 V board supply is used for the control units of the accelerator. The 200 V board supplies are used for the power supplies of the accelerator.

There is a 100 V–20 kVA board supply in the control room. It is used for the control units and the small power supplies for the focusing coils.

9. SCHEDULE

The construction of the 100 MeV electron injector has been finished. The tests of the main components such as the booster klystron, main klystron and the electron gun are performed now. The beam acceleration test is scheduled in spring 1995 and the beam quality will be measured and improved.

ACKNOWLEDGMENTS

The authors have grateful thanks to the Dr. Kobayashi and Dr. Shoji at JAERI for their advises about the electron linac. We also thank to Mr. Shoda and the staffs of the Nihon Kensetsu Kogyo Co Ltd. for their work. Mr. Kazama at ICR helped us for the construction and we would like to present our thanks to him.

REFERENCES

(1) A. Noda, *et al.*, "Design of the KSR", *Bulletin of the Institute for Chemical Research, Kyoto Univ.*, Vol. **73**, No.

1 (1995) (in press).
(2) H. Takekoshi, *et al.*, "Design, Construction and Operation of JAERI-Linac", *JAERI-Report*, **1238** (1975).
(3) K. Mashiko, *et al.*, JAERI-Memo, private communication.
(4) T. Shirai, *et al.*, "Study of the Beam Profile Monitor for the Proton Linac", *Bulletin of the Institute for Chemical Research, Kyoto Univ.*, Vol. **71**, No. 1, p. 15 (1993).